inorganics

MDPI

Article

The Silacyclobutene Ring: An Indicator of Triplet State Baird-Aromaticity

Rabia Ayub [1,2], Kjell Jorner [1,2] and Henrik Ottosson [1,2,*]

[1] Department of Chemistry—BMC, Uppsala University, Box 576, SE-751 23 Uppsala, Sweden; rabia.ayub@kemi.uu.se (R.A.); kjell.jorner@kemi.uu.se (K.J.)

[2] Department of Chemistry-Ångström Laboratory Uppsala University, Box 523, SE-751 20 Uppsala, Sweden

* Correspondence: henrik.ottosson@kemi.uu.se; Tel.: +46-18-4717476

Received: 23 October 2017; Accepted: 11 December 2017; Published: 15 December 2017

Abstract: Baird's rule tells that the electron counts for aromaticity and antiaromaticity in the first ππ* triplet and singlet excited states (T_1 and S_1) are opposite to those in the ground state (S_0). Our hypothesis is that a silacyclobutene (SCB) ring fused with a [4*n*]annulene will remain closed in the T_1 state so as to retain T_1 aromaticity of the annulene while it will ring-open when fused to a [4*n* + 2]annulene in order to alleviate T_1 antiaromaticity. This feature should allow the SCB ring to function as an indicator for triplet state aromaticity. Quantum chemical calculations of energy and (anti)aromaticity changes along the reaction paths in the T_1 state support our hypothesis. The SCB ring should indicate T_1 aromaticity of [4*n*]annulenes by being photoinert except when fused to cyclobutadiene, where it ring-opens due to ring-strain relief.

Keywords: Baird's rule; computational chemistry; excited state aromaticity; Photostability

1. Introduction

Baird showed in 1972 that the rules for aromaticity and antiaromaticity of annulenes are reversed in the lowest ππ* triplet state (T_1) when compared to Hückel's rule for the electronic ground state (S_0) [1–3]. The rule has subsequently been confirmed by a series of quantum chemical calculations [3,4], and it has also been shown that 4*n* π-electron species can have triplet multiplicity ground states (T_0). Interestingly, the T_0 state cyclopentadienyl cation and the isomeric vinylcyclopropenium cation (a closed-shell singlet) are nearly isoenergetic [5,6], revealing that Baird-aromatic stabilization of triplet state species can be significant [3,7]. It has also been shown through computations that Baird's rule can be extended to the lowest ππ* excited singlet states (S_1) of cyclobutadiene (CBD), benzene, and cyclooctatetraene (COT) [8–13]. Thus, [4*n*]annulenes display aromatic character in both their T_1 (or T_0) and S_1 states whereas [4*n* + 2]annulenes display anti-aromaticity. With Hückel's and Baird's rules it becomes clear that benzene has a dual character and can be labelled as a molecular "Dr. Jekyll and Mr. Hyde" [3,14,15]. This is in line with the early conclusions by Baird as well as by Aihara [1,16], and the excited state antiaromaticity explains the photoreactivity of many benzene derivatives [14]. On the other hand, CBD and COT are both aromatic in the T_1 state [17–19].

In the last few years, the excited state aromaticity and antiaromaticity concepts (abbr. ES(A)A) have gained gradually more attention [20–22], even though the pioneering experimental studies were presented by Wan and co-workers already in the 80s and 90s [23–28]. We earlier stressed that Baird's rule can be used as a qualitative back-of-an-envelope tool for the design of photochemically active materials, as well as for the development of new photoreactions [29,30]. Indeed, a recent combined experimental and computational study of a chiral thiopheno-fused COT compound by Itoh and co-workers reveals that the aromatic stabilization energies in both the T_1 and S_1 states are extensive (~21 kcal/mol) [31], in agreement with previous computational estimates of T_1 state (anti)aromatic

(de)stabilization [32,33]. For experimental identification of excited state aromatic cycles vs. anti- and nonaromatic ones, there is a need for suitable indicator moieties. Based on both computations and experiments we recently reported that the cyclopropyl (cPr) group can differentiate T_1 and S_1 state aromatic rings from those that are antiaromatic or nonaromatic in these states [34]. Yet, the cPr group also has a drawback in that the products formed upon ring-opening are not easily identified as they are complicated mixtures or polymeric material.

Herein, we discuss a computational study on the effects of T_1 state (anti)aromaticity of [4*n*]- and [4*n* + 2]annulenes on the photochemical ring-opening of a silacyclobutene (SCB) ring fused with an annulene. The SCB ring is interesting because of its ring-strain and high chemical reactivity [35]. One could potentially use the SCB ring as a substituent on an annulene ring, and here it is already known that 1,1-dimethyl-2-phenyl-1-silacyclobut-2-ene ring-opens photochemically [36], likely a route for excited state antiaromaticity relief. However, when used as a substituent the opening of the SCB ring will also be affected by conformational factors (Figure 1a). Instead, if fused it sits in the same arrangement regardless of annulene, and thus, should be a more unbiased indicator (Figure 1b).

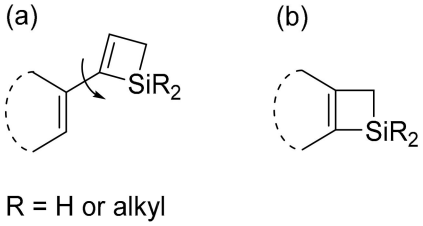

Figure 1. The silacyclobutene (SCB) ring as a substituent (**a**) and fused to an annulene ring (**b**).

We argue that the T_1 aromaticity of [4*n*]annulenoSCBs will hinder the SCB ring from opening as this will lead to loss of T_1 aromaticity, while the T_1 antiaromaticity of [4*n* + 2]annulenoSCBs instead will enhance the rate for ring-opening. We base this argument on the Bell–Evans–Polanyi principle that says that the activation energy will be proportional to the reaction energy for reactions of the same type [37]. This will lead to a photoreactivity difference which can allow the SCB ring to function as a T_1 aromaticity indicator. Noteworthily, the T_1 state potential energy surfaces (PESs) for electrocyclization reactions of compounds with 4*n* π-electrons were earlier explored by Mauksch and Tsogoeva [38], and Möbius aromatic transition states were identified in compounds with 8, 10 and 12π-electrons. Yet, the focus of our paper is not on the T_1 state electrocyclic ring-opening of SCB but instead on the explicit effect of the T_1 state (anti)aromaticity of annulenes on the SCB ring-opening when these annulenes are fused to the SCB ring. Earlier, we reported that the shapes of T_1 state PESs for twists about the C=C double bonds (cf. T_1 state *Z*/*E*-isomerizations) of [4*n*]- and [4*n* + 2]annulenyl substituted olefins are connected to changes in T_1 state (anti)aromaticity of (hetero)annulenyl substituents [39–42]. From this, one can infer that the T_1 state PES of also other photoreactions will vary in dependence of a neighboring [4*n* + 2]- or [4*n*]annulene ring. BenzoSCB (**2a**, Figure 2) should photorearrange to *o*-silaxylylene (**2b**), containing a highly reactive Si=C double bond [43], while cyclobuteno-(**1a**) and cyclooctatetraenoSCB (**3a**), based on our hypothesis, should be resistant to photochemical ring-openings. Indeed, photochemical ring-opening of **2a** in the S_1 state to the transient **2b**, trapped by alcohol solvents to yield isolable silylethers in 40–80% yield (Scheme 1), was earlier reported by Kang and co-workers [44]. Additions of alcohols to silenes, particularly naturally polarized ones ($Si^{\delta+}=C^{\delta-}$), proceed over very low activation barriers (a few kcal/mol) [45] due to the high oxy- and electrophilicity of the sp^2 hybridized Si atom, making these reactions highly suitable for rapid trapping of transient SCB ring-opened isomers. A potential benefit of the SCB ring over the cyclopropyl group is the persistence of the products formed upon photochemical SCB ring-opening followed by trapping [44,46].

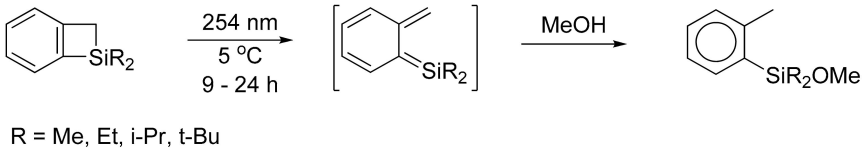

Scheme 1. The photochemical SCB ring-opening and subsequent trapping of *ortho*-silaxylylene reported by Kang, K.T. et al. [44].

Our investigation is focused on the T_1 state ring-openings rather than the S_1 state processes as the triplet states are more easily amenable to computations. We used different aromaticity indices to examine the (anti)aromatic character of ring-closed and ring-opened isomeric structures. If T_1 aromaticity of a [4*n*]annulene hinders the SCB ring from opening, then the absence of this reaction upon irradiation should indicate T_1 aromaticity. The SCB ring-opening could tentatively be connected to the bond dissociation enthalpies (BDEs) because the C–C BDE in a strain-free compound (90.4 kcal/mol) is slightly higher than the Si–C BDE (88.2 kcal/mol), which in turn is higher than the Si–Si (80.5 kcal/mol) BDE [47,48]. Although the BDE difference between the strain-free C–C and Si–C bonds is small, strain could be more important in the SCB ring than in the all-carbon cyclobutene ring (vide infra). Here it can be noted that the cyclobutene and disilacyclobut-3-ene rings are less suitable than the SCB ring because the former opens only rarely upon photolysis (e.g., benzocyclobutene does not undergo photochemical ring-opening unless further derivatized) [14,49], while the latter is unstable and readily oxidized in air to 1,3-disila-2-oxacyclopentenes [50]. It should also be noted that strained four-membered rings with heteroatoms from Groups 15 and 16 are problematic in the context of excited state aromaticity indicators as these heteroatoms provide lone-pair electrons that will interact electronically with the π-conjugated annulene. Additionally, the lowest excited states of compounds with such rings could be of nπ* rather than of ππ* character, leading to excited states for which Baird's rule is not applicable. The SCB ring when used as a substituent can also influence the annulene through π-conjugation, yet, when fused onto an annulene its C=C bond is joint with the annulene. Thus, the SCB ring could hold a unique position as a tentative excited state aromaticity indicator unit.

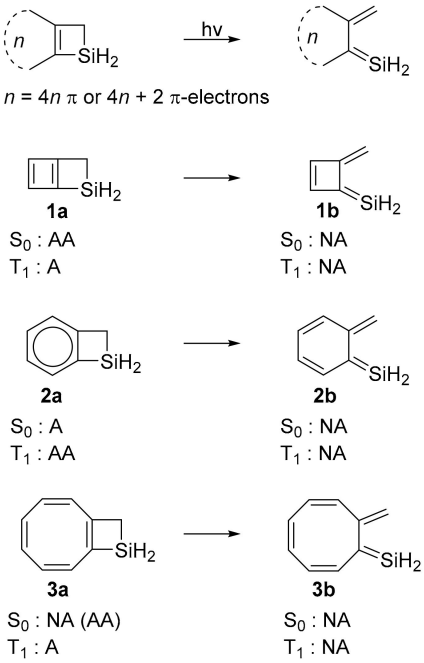

Figure 2. The annulenoSCB ring-openings and the postulated (anti)aromatic characters in the S_0 and the T_1 states of **1a**, **2a**, **3a**, **1b**, **2b**, and **3b**, respectively, with A = aromatic, AA = antiaromatic, and NA = non-aromatic.

2. Results and Discussion

We first discuss the changes in energies, geometries and (anti)aromaticities in the T_1 states during ring-opening reactions of the three molecules (Figure 2) in which a SCB ring is fused with either a [4*n*]annuleno-(cyclobuteno- and cyclooctatetraeno-) ring or a [4*n* + 2]annuleno-(benzo-) ring. We discuss reaction and activation energies, and subsequently analyze (anti)aromaticity changes through the harmonic oscillator model of aromaticity (HOMA), nucleus independent chemical shift (NICS) and isomerization stabilization energy (ISE) indices as well as anisotropy of the induced current density (ACID) plots. Finally, openings of SCB rings fused with 5- and 7-membered annulenyl cations and anions are discussed. We also explored the T_1 PES for SCB ring-opening when fused with polycyclic systems (see Scheme S1), and for comparison the all-carbon analouges of **2** and **3** were analyzed.

2.1. Energy Changes

For the first three compounds (**1**–**3**), three different methods, two density functional theory methods (B3LYP and OLYP), and one Coupled Cluster method (CCSD(T)) were tested to ensure that the results do not vary extensively with method. Similar results were mostly obtained at the two DFT (B3LYP and OLYP) and CCSD(T) levels, and therefore, only B3LYP energies are given for the remaining compounds unless otherwise noted. Compound **2a**($\mathbf{T_1}$) had a higher relative energy than that of its ring-opened isomer, **2b**($\mathbf{T_1}$), by 33.7–38.3 kcal/mol depending on the computational method (Figure 3). Moreover, the activation energy for Si–C bond scission in the T_1 state was merely 9.0 kcal/mol, 38.3 kcal/mol lower than in the S_0 state at the B3LYP level. This suggests that an antiaromatic destabilization of the benzene ring in the T_1 state affected **2a**($\mathbf{T_1}$) making it highly unstable and prone to cleave the Si–C bond.

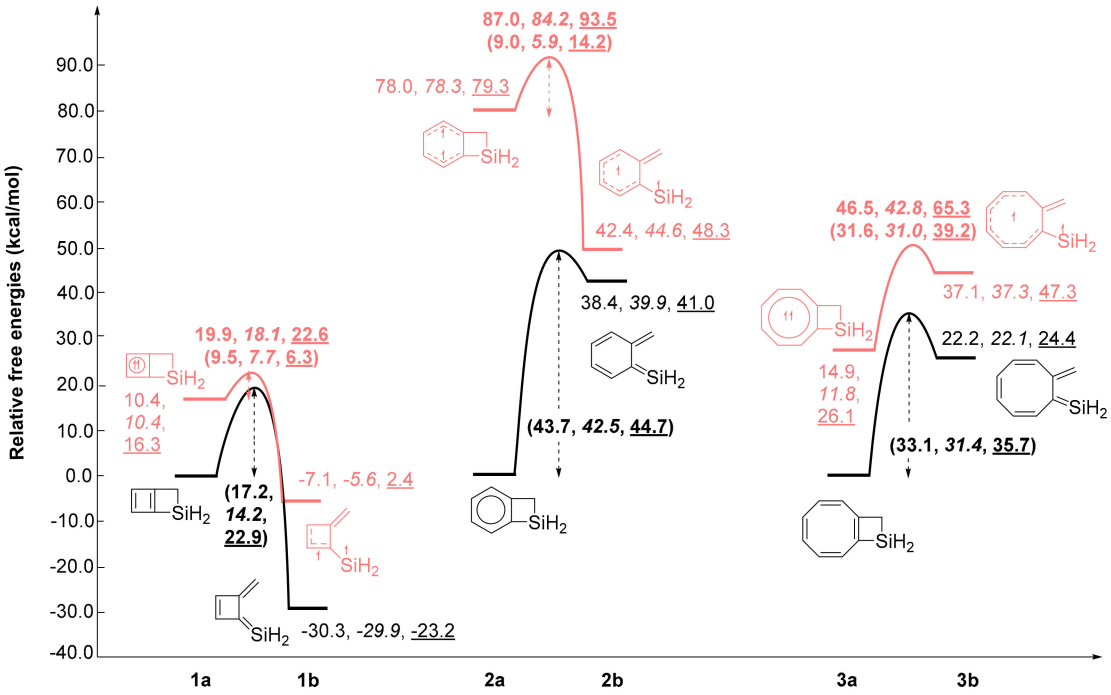

Figure 3. T_1 state potential free energy surface diagrams for ring-openings of 2,3-cyclobutadieno-1-SCB (**1**), 2,3-benzo-1-SCB (**2**) and 2,3-cyclooctatetraeno-1-SCB (**3**) at (U)B3LYP/6-311G(d,p) (normal print), (U)OLYP/6-311G(d,p) (italics), and (U)CCSD(T)/6-311G(d,p)//(U)B3LYP/6-311G(d,p) (underlined) levels. Values in parenthesis are activation energies. Values for the S_0 state in black and values for the T_1 state in red.

Interestingly, the T_1 PES of **1** displayed a similar shape as that of **2**, since **1b**(**T_1**) is of lower energy than **1a**(**T_1**) despite the fact that CBD is weakly T_1-aromatic [8,13,17,51–53]. At the two DFT levels, **1b**(**T_1**) was even lower than **1a**(**S_0**), likely due to ring-strain relief in **1b**(**T_1**). Furthermore, the activation energy in the T_1 state was lower than that in the S_0 state by 7.7 kcal/mol at B3LYP level. An opposite behavior was observed for **3** in its T_1 state because **3b**(**T_1**) is higher in energy than **3a**(**T_1**) by 11.8–26.1 kcal/mol. Moreover, the activation energies in the T_1 state are very high, 31.0–39.2 kcal/mol, revealing that the SCB ring will remain closed. Thus, for compounds **2** and **3**, the energy changes upon ring-opening in the T_1 states fell in line with our hypothesis; ring-opening releases energy in **2** in the T_1 state, while it requires energy in **3**. The question was, to what extent these energy changes were linked to changes in (anti)aromaticity (vide infra).

The Si–C bond lengths in **1a**, **2a**, and **3a** are 1.95 Å, 1.92 Å, and 1.90 Å, respectively, which is slightly longer than the normal Si–C bond length (1.87–1.89 Å) [54]. Thus, as one goes to gradually larger annulene rings, the SCB ring gets successively less strained when evaluated based on Si–C bond lengths.

Noteworthily, in the S_0 state, the reaction energy for ring-opening of **2a**(**S_0**) was of opposite sign to the reaction energy in the T_1 state. This reversal in endergonicity and exergonicity when going from the S_0 to the T_1 state of **2** should be a consequence of Baird's rule being the exact opposite to Hückel's rule. With regard to compounds **1** and **3** in the S_0 states, the ring-opening of **1a**(**S_0**) was exergonic, in line with relief of both S_0 antiaromaticity and ring-strain, while ring-opening in the non-aromatic isomer **3a**(**S_0**) was endergonic. These energies were a combination of factors; (i) changes in (anti)aromaticity, (ii) ring strain release, and (iii) changes in the bonding character at the Si atom as it goes from sp^3 to sp^2 hybridized. Formation of a Si=C double bond is an unfavorable process which is not sufficiently compensated by relief of ring strain in the least ring strained of the compounds (**3a**(**S_0**)). Indeed, the ring opening of the all-carbon congener (**allC-3**(**S_0**)), where a C=C double bond is formed instead, was exergonic by 6.4 kcal/mol (see Figure S13).

For **2** and **allC-2**, the S_0 electrocyclic ring-opening transition states were conrotatory, as expected for a thermal reaction with $4n$ electrons. In T_1, this was reversed to a disrotatory fashion. In contrast, for **3** and **allC-3**, both the S_0 and T_1 transition states were conrotatory. The conrotatory mode in T_1 could be explained by the fact that the spin density is delocalized both over the eight-membered and four-membered rings in the TS (Figures S44 and S45). This is consistent with a 10-electron electrocyclic ring-opening with Möbius orbital topology which would be allowed in T_1. Indeed, the ACID plots for **3** and **allC-3** supported this interpretation, as the ring current went over all 10 atoms (Figures S54 and S55). However, the difference of mechanism in T_1 with 10-electron conrotatory for **3** and 4-electron disrotatory for the other molecules was not sufficiently large to prevent application of the Bell–Evans–Polanyi principle, as they all fell on the same correlation line (Figure S40, vide infra).

In addition to the SCB ring fused to aromatic and antiaromatic annulenes, we also analyzed it when fused to the non-aromatic reference compounds cyclobutene, cyclohexene, and cyclohexadiene. When going from **4** to **6** over **5**, the reaction energies in the T_1 state became gradually less strongly exergonic, while the activation energies increased slightly. Compounds **4** and **5** both have nonconjugated C=C double bonds, yet, the cycloalkene ring was larger in **5**, leading to less ring-strain than in **4**, as well as a T_1 state SCB ring-opening reaction energy which was lower by 11.3 kcal/mol. When going from **5** to **6**, the reaction energy further decreased by 12.1 kcal/mol, revealing that the length of the conjugated path also had an impact. An indication that T_1 state antiaromaticity was alleviated in **2a**(**T_1**) was the fact that the energy released when going from **2a**(**T_1**) to **2b**(**T_1**) (Figure 3) was larger than when going from **5a**(**T_1**) to **5b**(**T_1**) (Figure 4). Indeed, the ring-closed **2a**(**T_1**) was at an even higher energy than **5a**(**T_1**) where the triplet biradical was confined to an essentially planar olefin bond. This clarified that the benzene ring in the T_1 state was strongly destabilized. The destabilized nature of T_1 state benzene became obvious when regarding compound **6,** where the ring-closed isomer has a SCB moiety with its C=C double bond being part of a conjugated, yet, nonaromatic segment because the T_1 energy of **2a**(**T_1**), was substantially higher than that of **6a**(**T_1**) (78.0 vs. 47.5 kcal/mol,

respectively). Moreover, the activation energy for SCB ring-opening of **2a**($\mathbf{T_1}$) was 6.6 kcal/mol lower than that of **6a**($\mathbf{T_1}$), which indicated an influence of T_1 antiaromaticity in **2a**($\mathbf{T_1}$).

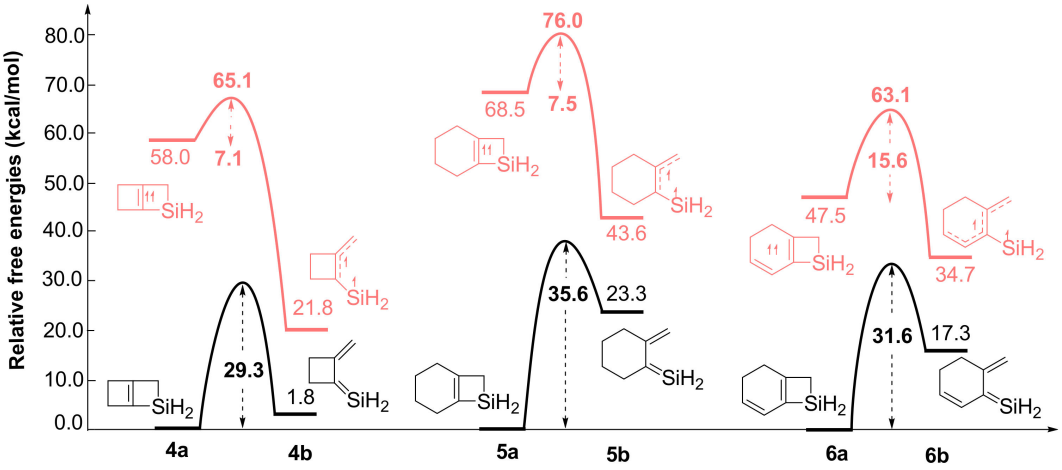

Figure 4. Relative reaction and activation free energies (kcal/mol) for the SCB ring-opening when fused to non-aromatic rings. The energies for transition states are given in bold. Black energy levels represent the S_0 state and red ones represent T_1 states at (U)B3LYP/6-311G(d,p) level.

2.2. Changes in T_1 State (Anti)aromaticity upon Ring-Opening

2.2.1. Harmonic Oscillator Model of Aromaticity (HOMA) Values

Bond length equalization is one indicator of aromaticity, and we chose the geometric HOMA index as one of the indices used (Table 1). The large negative HOMA values in **1a**($\mathbf{S_0}$), **1b**($\mathbf{S_0}$) and **1b**($\mathbf{T_1}$) corresponded to antiaromaticity, while the small HOMA value of **1a**($\mathbf{T_1}$) suggested that this structure is non-aromatic. Ring-opening of **1a**($\mathbf{T_1}$) to **1b**($\mathbf{T_1}$) led to an increase in antiaromaticity (ΔHOMA(T_1) = −0.69).

Table 1. Harmonic oscillator model of aromaticity (HOMA) values at the (U)B3LYP/6-311G(d,p) level of compounds **1**, **2**, and **3**.

Compounds	$\mathbf{S_0}$			$\mathbf{T_1}$		
	a	**b**	**ΔHOMA**	**a**	**b**	**ΔHOMA**
1	−4.04	−1.11	2.93	0.10	−0.59	−0.69
2	0.97	0.07	−0.90	−0.32	0.83	1.15
3	0.08	−0.21	−0.13	0.89	0.21	−0.68

Compound **2**, in comparison, was aromatic in structures **2a**($\mathbf{S_0}$) and **2b**($\mathbf{T_1}$) while it was non-aromatic in structures **2a**($\mathbf{T_1}$) and **2b**($\mathbf{S_0}$). Since **2a**($\mathbf{T_1}$) is non-aromatic, ring-opening to **2b**($\mathbf{T_1}$) was favored, as aromaticity was gained (ΔHOMA(T_1) = 1.15). Benzene in the T_1 state can adopt several different conformers depending on the starting geometry; (i) it can have a quinoidal structure with two unpaired electrons in the *para*-positions and two double bonds parallel to the C_2-axis (^{3}**Q**), (ii) it can have an anti-quinoidal structure with two allyl radical segments (^{3}**AQ**), or (iii) it can be described as a combination of a pentadienyl and a methyl radical (^{3}**PM**) [55] (Figure 5). Isomer **2a**($\mathbf{T_1}$) is geometrically most similar to ^{3}**AQ** since it has two long CC bonds and two allylic segments (see Figure S9).

The small HOMA values of **3a**($\mathbf{S_0}$), **3b**($\mathbf{S_0}$) and **3b**($\mathbf{T_1}$) indicate that these are nonaromatic while a high positive value of **3a**($\mathbf{T_1}$) suggests aromatic character. Thus, ring-opening of **3** in the T_1 state entails an unfavorable reduction in aromaticity as ΔHOMA(T_1) = −0.68. Taken together, the HOMA

values support our hypothesis that T_1 state aromaticity is lost in SCB ring-openings of **1a** and **3a**, while the T_1 state antiaromaticity of **2a** is alleviated in this reaction.

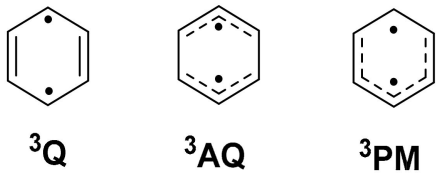

Figure 5. The quinoid (**Q**), anti-quinoid (**AQ**), and pentadienyl-methyl (**PM**) conformers of T_1-state benzene.

2.2.2. Nucleus Independent Chemical Shift (NICS) Scans

NICS is a magnetic indicator of aromaticity. The chemical shifts of NICS probe are scanned over a certain distance (0–5 Å) above the center of the molecular plane. The out-of-plane component obtained is then plotted against the distance. The NICS scans of **1**–**3** in their T_1 states in ring-closed and ring-opened isomers are shown in Figure 6, while those in the S_0 states are found in Figure S1. With regard to **1a**($\mathbf{T_1}$), the out-of-plane component in the NICS scan had a negative value (−14.4 ppm; 1.1 Å) suggesting that this structure is significantly aromatic. Conversely, a high positive value of the out-of-plane component in **1b**($\mathbf{T_1}$) shows that this structure had antiaromatic character. For **2**, it was found instead to be **2a**($\mathbf{T_1}$), as it had a high positive value for the out-of-plane component (90.9 ppm; 0 Å) revealing that this structure was T_1 antiaromatic. This T_1 antiaromaticity changed back to aromaticity when the SCB ring opened, because a value of −19.8 ppm at 1.1 Å was calculated for **2b**($\mathbf{T_1}$). With regard to **3**, the NICS scan showed **3a**($\mathbf{T_1}$) to be aromatic with a value of −30.4 ppm at 0.9 Å, yet, **3b**($\mathbf{T_1}$) was non-aromatic. Because of the non-planarity of the COT of **3b**($\mathbf{T_1}$) a small kink was observed in its NICS scan, in contrast to that of **3a**($\mathbf{T_1}$) (Figure 6 and Figure S1). Discontinuities in NICS-*XY* scans due to non-planarities were earlier observed by Schaffroth and co-workers for tetraazaacenes [56]. Thus, based on NICS, we have support for our hypothesis that T_1 (anti)aromaticity influences the reaction energies for the ring-openings of **1**, **2**, and **3**. This led to loss of T_1 aromaticity in **1** and **3**, whereas it leads to alleviation of T_1 antiaromaticity in **2**. This reversal when going from **1** to **2**, and then to **3** was also viewed clearly in Figure 6, since the structures with negative (aromatic) NICS values were successively **1a**($\mathbf{T_1}$), **2b**($\mathbf{T_1}$) and **3a**($\mathbf{T_1}$).

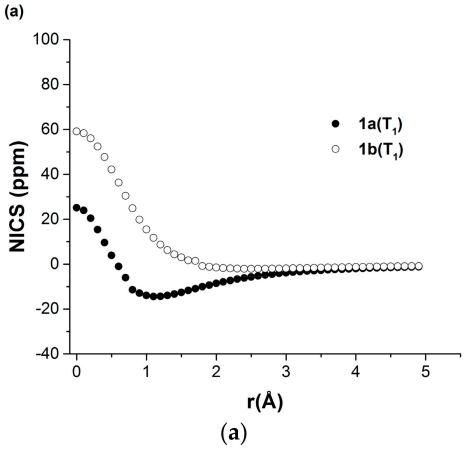

Figure 6. *Cont.*

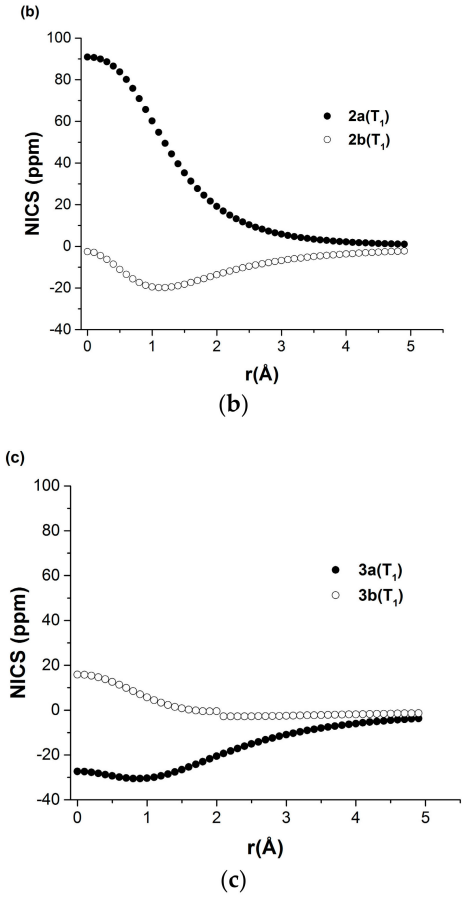

Figure 6. Nucleus independent chemical shifts (NICS) scans of (**a**) **1a**($\mathbf{T_1}$) and **1b**($\mathbf{T_1}$); (**b**) **2a**($\mathbf{T_1}$) and **2b**($\mathbf{T_1}$); as well as (**c**) **3a**($\mathbf{T_1}$) and **3b**($\mathbf{T_1}$) at the GIAO-(U)B3LYP/6-311+G(d,p)//(U)B3LYP/6-311G(d,p) level. Only the out-of-plane components are displayed.

2.2.3. Anisotropy of the Induced Current Density (ACID) Plots

ACID is a magnetic indicator of aromaticity for visualizing ring-currents and electron delocalization. The ACID plots (Figure 7) of compounds **1**, **2**, and **3** corroborated the results of the NICS scans. Clockwise ring-currents for **1a**($\mathbf{T_1}$), **2b**($\mathbf{T_1}$) and **3a**($\mathbf{T_1}$) indicated aromaticity, while counter-clockwise ring-currents in **1b**($\mathbf{T_1}$) and **2a**($\mathbf{T_1}$) represented antiaromaticity. Yet, the ring-currents in **1b**($\mathbf{T_1}$) suggested this structure to be only weakly antiaromatic. The **3b**($\mathbf{T_1}$) structure was non-aromatic. Clearly, **2a**($\mathbf{T_1}$) opened the SCB ring to alleviate T_1 antiaromaticity (a favorable process), while **1a**($\mathbf{T_1}$) and **3a**($\mathbf{T_1}$) lost aromaticity upon ring-openings (unfavorable processes).

2.2.4. Isomerization Stabilization Energy (ISE) Values

ISE is an energetic index of aromaticity and it is based on the energy difference between the calculated total energy of fully aromatic methyl isomer to that of the non-aromatic exocyclic methylene isomer. We also utilized the isomerization stabilization energy (ISE) index of Schleyer [32] to estimate either the aromaticity or antiaromaticity in ring-closed structures in the T_1 state. Here, we examined only **1** and **2**, and only in their T_1 states. With regard to the smallest compounds, the 4- and 5-methyl substituted **1a**($\mathbf{T_1}$) derivatives showed negative ISE values (ISE_{avg} −10.1 kcal/mol, Figure 8), indicative of some T_1 aromatic stabilization. With regard to **2**, the methyl-substituted **2a**($\mathbf{T_1}$) structures showed positive ISE values from 10.1 to 12.6 kcal/mol, indicative of T_1 antiaromatic destabilization. Structure **2a**($\mathbf{T_1}$) is highly destabilized, evident from the computed ISE values. On the other hand, the ISE values

reported for benzene in S_0 state is −33.2 kcal/mol [57]. Thus, the ISE values support our hypothesis that **2a**($\mathbf{T_1}$) is destabilized to the same extent as **1a**($\mathbf{T_1}$) is stabilized.

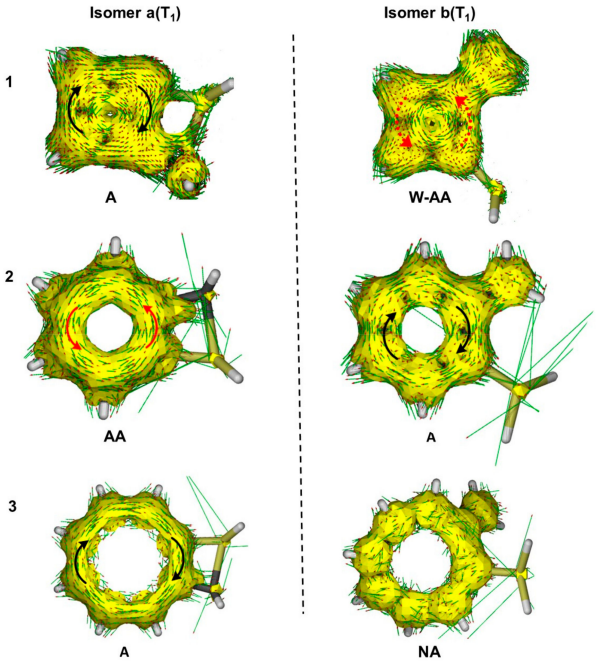

Figure 7. Anisotropy of the induced current density (ACID) plots at (U)B3LYP/6-311+G(d,p)//(U)B3LYP/6-311G(d,p) level. Broken arrows in **1b**($\mathbf{T_1}$) indicate weaker ring-currents. Aromatic = A, antiaromatic = AA, weakly antiaromatic = WAA, and non-aromatic = NA.

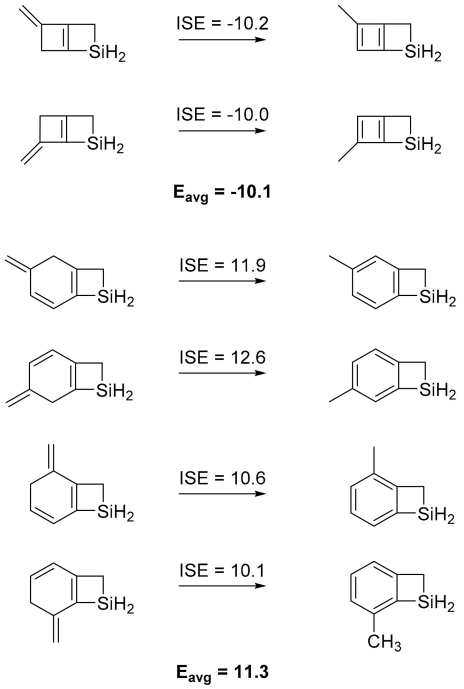

Figure 8. Isomerization stabilization energy (ISE) values (kcal/mol) of the 4- and 5-methyl substituted **1a**($\mathbf{T_1}$) derivatives, and the 5-, 6-, 7-, and 8-methyl substituted **2a**($\mathbf{T_1}$) derivatives at the UB3LYP/6-311G(d,p) level. ISE_{avg} is the average ISE value for the various methyl substitutions.

2.3. Five- and Seven-Membered Carbocyclic Anions and Cations Fused to SCB

In order to explore if the findings on **1**–**3** can be extended to other [4*n*]- and [4*n* + 2]annulenyl-SCBs, we examined the potential energy surfaces of 5- and 7-membered annulenyl cations and anions fused to SCB rings (**7**–**9**, Figure 9). This also allowed us to evaluate how the reaction energies depend on the annulene size. It should be noted that we only investigated energy and geometry changes, and we predicted **7** and **9** to resemble **1** and **3**, respectively, while **8** should resemble **2**. The SCB-fused Cp- was excluded as its calculated T_1 state was of $\pi\sigma^*$ and not of $\pi\pi^*$ character.

The **7a**($\mathbf{S_0}$) structure was a transition state; being a 4π-electron species it is strongly singlet state antiaromatic, it showed large CC bond length alternations (Figure S11), and it was unstable to SCB ring-opening, leading to singlet state antiaromaticity alleviation. On the other hand, **7a**($\mathbf{T_1}$) in the T_1 state was a minimum on the T_1 PES; its geometry met the aromaticity criterion of bond length equalization, and the spin density was uniformly distributed over the cyclopentadienyl fragment (Figure S12). Interestingly, it was 2.9 kcal/mol lower in energy than **7a**($\mathbf{S_0}$), similar to the parent cyclopentadienyl cation which has a triplet ground state [58–61]. The ring-opening of **7a**($\mathbf{T_1}$) to **7b**($\mathbf{T_1}$) was endergonic by 3.8 kcal/mol, opposite to the ring-opening of **1a**($\mathbf{T_1}$) to **1b**($\mathbf{T_1}$) which was exergonic by 17.5 kcal/mol. The reason why **1a**($\mathbf{T_1}$) does not behave similar to **7a**($\mathbf{T_1}$) and **3a**($\mathbf{T_1}$) could be explained by the ring-strain in the CBD ring.

With regard to **9a**($\mathbf{T_1}$), it was merely 4.2 kcal/mol higher in energy than **9a**($\mathbf{S_0}$), and its geometry indicated a completely delocalized cycloheptatrienyl anion. This delocalization of the triplet biradical character was also confirmed through its spin density (Figure S12). The ring-opening of **9a**($\mathbf{T_1}$) to **9b**($\mathbf{T_1}$) was energetically unfavorable, yet, not equally unfavorable as the ring-opening of **3a**($\mathbf{T_1}$) to **3b**($\mathbf{T_1}$). Thus, when going to gradually larger annulenes the SCB ring-opening energies in the T_1 state were −17.5 (**1**), 3.8 (**7**), 12.2 (**9**), and 22.2 (**3**) kcal/mol, respectively. i.e., only the most ring-strained compound (**1**) displayed an exergonic reaction energy. The activation energies in the T_1 state also increased gradually and they were 9.5 (**1**), 21.7 (**7**), 24.6 (**9**) and 31.6 (**3**) kcal/mol, respectively. Hence, the SCB ring, when fused with [4*n*]annulenes will in general not open in the T_1 state, a feature that stems from T_1 aromaticity. When an SCB ring is attached to an annulene ring, the absence of a photochemical ring-opening should therefore indicate T_1 aromaticity. Only when ring-strain is high, as in **1a**($\mathbf{T_1}$), will T_1 state ring-opening occur in such species.

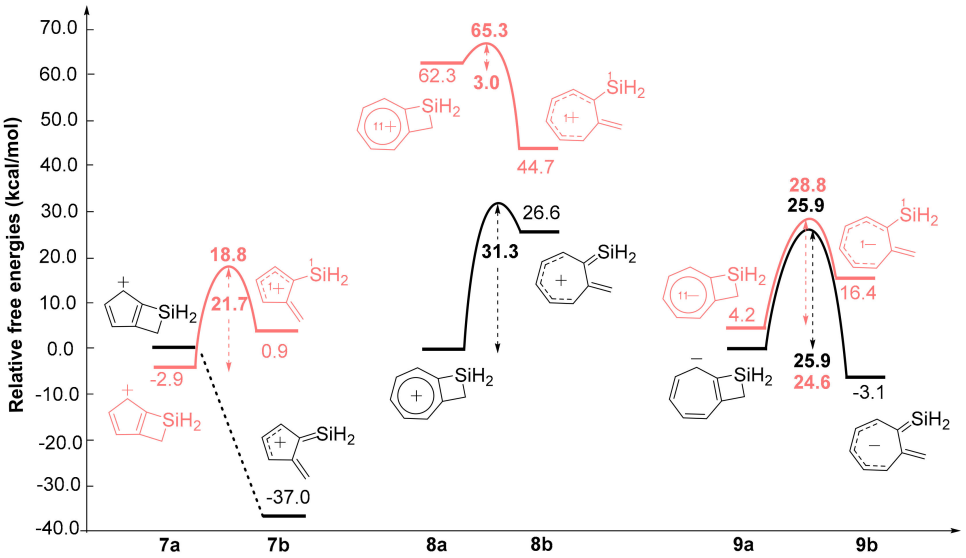

Figure 9. Free energy changes in 5- and 7-membered annulenyl cations and anions fused with SCB rings upon ring-openings at (U)B3LYP/6-311G(d,p) level. Compound **7a**($\mathbf{S_0}$) is not a minimum in the S_0 state. The black energy levels represent S_0 and those of red indicate T_1 state and energies for transition states are given in bold.

Compound **8** showed the opposite behavior to that found for **7** and **9**. Structure **8a**($\mathbf{T_1}$) was highly skewed and its ring-opening to **8b**($\mathbf{T_1}$) was exergonic by 17.6 kcal/mol. Also, the ring-opened **8b**($\mathbf{T_1}$) isomer was planar and had a CC bond delocalized structure. Thus, **8** having a [4*n* + 2]annulene moiety, displayed similar characteristics as **2**. Yet, the smaller the ring, the higher the exergonicity of the ring-opening, explained by relief of ring-strain in addition to the relief of T_1 antiaromaticity. Taken together, the T_1 state ring-opening reactions were markedly uphill for compounds **3**, **7**, and **9**, and downhill for **2** and **8**. Compounds **3**, **7**, and **9** showed T_1 aromaticity similar to [4*n*]annulenes, while compounds 2 and 8 showed T1 antiaromaticity analogous to [4*n* + 2]annulenes, suggesting that loss of T1 aromaticity was observed in ring-openings of [4*n*]annulenes while T1 antiaromaticity of [4*n* + 2]annulenes is alleviated through such reactions. Finally, the T1 state activation energies for SCB rings of the T1 aromatic compounds 3, 7, and 9 were higher than those of the non-aromatic reference compounds **4**–**6** (Figure 10), allowing the SCB ring to function as a T_1 state aromaticity indicator. For the (4*n* + 2)π-electron annulenoSCBs, the activation energies were similar or lower than those of the nonaromatic references. Overall, the height of the activation barriers in the T_1 state were, to a significant extent, correlated with the reaction energies (R^2 = 0.762, Figure S40), in accordance with the Bell–Evans–Polanyi principle. This correlation was even stronger for the S_0 state (R^2 = 0.872).

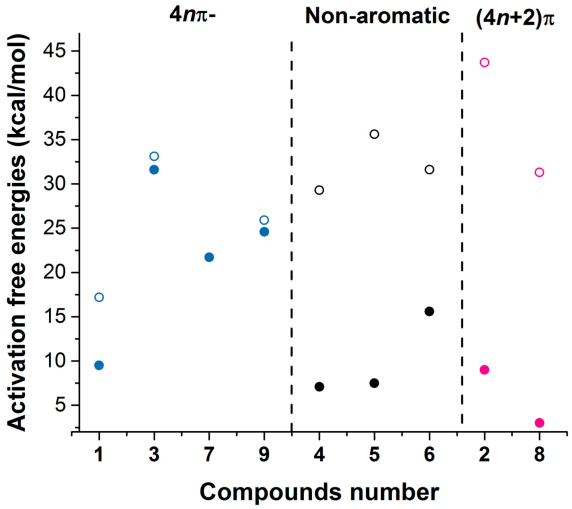

Figure 10. Activation free energies (kcal/mol) of all compounds **1**–**9** at the (U)B3LYP/6-311G(d,p) level in the S_0 (unfilled circles) and T_1 (filled circles) states.

2.4. Polycyclic Structural Units Fused to SCB

In order to test the generality of the hypothesis, the reaction and activation energies for the ring-opening of an SCB ring when fused to polycyclic moieties (10 and 12π-electrons) were also explored (Scheme S1). With 10 π-electrons, naphthalene is T_1 antiaromatic, and we found that the SCB ring-openings of all three isomers of naphtho-SCB (**10a**–**10c**) were exergonic, in line with our hypothesis. However, the activation energy for **10a** (23.3 kcal/mol) is significantly higher than observed for the cPr-naphthalenes previously studied (8–11 kcal/mol) [34], suggesting that the SCB ring will remain closed when fused to naphthalene. With regard to biphenylene, a 12π-electron compound which is T_1 state Baird-aromatic, the SCB ring-opening energies of **11a**–**11c** were modestly exergonic. Moreover, the activation barrier for SCB ring-opening was nearly the same as that of naphthalene (24.2 kcal/mol). Yet, it should be noted that polycyclic systems are more complex than monocycles because the SCB ring-opened products can adopt aromaticity in some of the rings leading to stabilization, a feature already observed for the ring-openings of the corresponding cPr substituted systems. Clearly, the SCB ring should remain closed for T_1 aromatic polycyclic compounds, however, it may also not open for polycyclic T_1 antiaromatic species, leading to limitations of its usage.

3. Computational Methods

All calculations were performed with Gaussian 09 revision D.01 [62]. The structures were optimized at the (U)B3LYP and (U)OLYP density functional theory levels [63–66], with the 6–311G(d,p) basis set [67,68]. Frequency calculations were carried out at the same level to confirm stationary points with real frequencies. Single-point energy calculations were performed at the (U)CCSD(T)/6-311G(d,p)//(U)B3LYP/6-311G(d,p) level and thermal corrections at the B3LYP level were added to get the free energies. Structural, magnetic and energetic indices were used to assess the extent of aromaticity [69]. The harmonic oscillator model of aromaticity (HOMA) [70] values were calculated at the (U)B3LYP/6-311G(d,p) level. Positive values approaching 1.0 correspond to aromatic compounds, negative values to antiaromatic compounds, and values close to zero indicate nonaromatic compounds. Nucleus independent chemical shift (NICS) scans along an axis perpendicular (*z*-axis) to the ring planes were generated with the Aroma package 1.0 [71–73], using the Gauge-Independent Atomic Orbital (GIAO) method [74] at the GIAO-(U)B3LYP/6-311+G(d,p)//(U)B3LYP/6-311G(d,p) level. Scans were performed starting at the centre of the annulene to 5.0 Å above the ring plane with increments of 0.1 Å. For aromatic compounds, the out-of-plane components show relatively deep minima. For non-aromatic compounds, the values close to the molecular plane are positive, decreases asymptotically and approach zero as the distance is increased. The antiaromatic compounds display high positive values for the out-of-plane components which go to zero with increasing distance. The anisotropy of the induced current density (ACID) calculations [75,76] were used to analyze the ring-currents with the CGST method [77] at (U)B3LYP/6-311+G(d,p) level with AICD 2.0.0 software package. The ACID plots were generated using (NMR = CGST IOp(10/93 = 1) and ultrafine grid (integral = grid = ultrafine). Clock-wise ring-currents indicates aromaticity and counter clock-wise ring-currents indicates antiaromaticity. Isomerization stabilization energies (ISE) [32,33,57] were calculated at the (U)B3LYP/6-311G(d,p) level.

4. Conclusions

We have shown that the ring-opening ability of the SCB ring in the T_1 state can be used to sense for T_1 aromaticity of a [4*n*]annulene to which it is fused, as its ring-opening disrupts the T_1 aromaticity of the [4*n*]annulene, an unfavorable (endergonic) process. Conversely, it should open regardless if fused to a T_1 non-aromatic or T_1 antiaromatic ring. By usage of a variety of (anti)aromaticity indices, we link the shapes of the T_1 PES to changes in T_1 (anti)aromaticity. Consequently, the SCB ring could be used as a T_1 aromaticity probe, in contrast to the all-carbon cyclobutene or disilacyclobutene rings which are either too photoresistent or too labile. Moreover, as the silacyclobutene ring when fused does not π-conjugate with the annulene, it has a benefit when compared to strained four-membered rings with Group 15 and 16 elements. The SCB ring also has a benefit over the cPr group examined earlier by us in the context of excited state aromaticity indicators [34] because the transient intermediate formed upon SCB ring-opening, in contrast to the ring-opened cPr intermediate, is easily trapped by alcohols to yield photostable silylethers. Yet, the SCB ring is likely of limited applicability in polycyclic systems as it may remain closed regardless of whether the ring system is T_1 aromatic or T_1 antiaromatic. Still, our study can be interesting from an applications perspective as it reveals situations when the SCB ring as a part in a larger molecule could lead to photoinstability of compounds used for various applications in organic electronics [78].

Supplementary Materials: The following are available online at www.mdpi.com/2304-6740/5/4/91/s1, NICS scans, ACID plots, geometries, spin densities, and Cartesian Coordinates.

Acknowledgments: We thank the EXPERTS III (Erasmus Mundus Action II program) and the Swedish Research Council (VR) for financial support. We also thank the SNIC and UPPMAX for generous allotment of computer time.

Author Contributions: Henrik Ottosson conceived the project and Henrik Ottosson and Rabia Ayub designed the project. Rabia Ayub performed most of the Quantum Chemical calculations. Kjell Jorner performed the calculations of the transition states. Rabia Ayub, Kjell Jorner and Henrik Ottosson co-wrote the manuscript.

Conflicts of Interest: The authors declare no conflict of interest.

References

1. Baird, N.C. Quantum Organic Photochemistry. II. Resonance and Aromaticity in the Lowest $^3\pi\pi^*$ State of Cyclic Hydrocarbons. *J. Am. Chem. Soc.* **1972**, *94*, 4941–4948. [CrossRef]
2. Ottosson, H. Organic Photochemistry: Exciting Excited State Aromaticity. *Nat. Chem.* **2012**, *4*, 969–971. [CrossRef] [PubMed]
3. Rosenberg, M.; Dahlstrand, C.; Kilså, K.; Ottosson, H. Excited State Aromaticity and Antiaromaticity: Oppertunities for Photophysical and Photochemical Rationalizations. *Chem. Rev.* **2014**, *114*, 5379–5425. [CrossRef] [PubMed]
4. Gogonea, V.; Schleyer, P.R.; Schreiner, P.R. Consequences of Triplet Aromaticity in $4n\pi$-Electron Annulenes: Calculation of Magnetic Shieldings for Open-Shell Species. *Angew. Chem. Int. Ed.* **1998**, *37*, 1945–1948. [CrossRef]
5. Glukhovtsev, M.N.; Reindl, B.; Schleyer, P.R. What is the Preferred Structure of the Singlet Cyclopentadienyl Cation? *Mendeleev Commun.* **1993**, *3*, 100–102. [CrossRef]
6. Glukhovtsev, M.N.; Bach, R.D.; Laiter, S. Computational Study of the Thermochemistry of $C_5H_5^+$ Isomers: Which $C_5H_5^+$ Isomer is the Most Stable? *J. Phys. Chem.* **1996**, *100*, 10952–10955. [CrossRef]
7. Mauksch, M.; Tsogoeva, S.B. A New Architecture for High Spin Organics based on Baird's rule of 4*n* Electron Triplet Aromatics. *Phys. Chem. Chem. Phys.* **2017**, *19*, 4688–4694. [CrossRef] [PubMed]
8. Karadakov, P.B. Ground- and Excited-State Aromaticity and Antiaromaticity in Benzene and Cyclobutadiene. *J. Phys. Chem. A* **2008**, *112*, 7303–7309. [CrossRef] [PubMed]
9. Karadakov, P.B. Aromaticity and Antiaromaticity in the Low-Lying Electronic States of Cyclooctatetraene. *J. Phys. Chem. A* **2008**, *112*, 12707–12713. [CrossRef] [PubMed]
10. Karadakov, P.B.; Hearnshaw, P.; Horner, K.E. Magnetic Shielding, Aromaticity, Antiaromaticity, and Bonding in the Lowest Lying Electronic States of Benzene and Cyclobutadiene. *J. Org. Chem.* **2016**, *81*, 11346–11352. [CrossRef] [PubMed]
11. Kataoka, M. Magnetic Susceptibility and Aromaticity in the Excited States of Benzene. *J. Chem. Res.* **2004**, *2004*, 573–574. [CrossRef]
12. Haas, Y.; Zilberg, S. The $\nu_{14}(b_{2u})$ Mode of Benzene in S_0 and S_1 and the Distortive Nature of the π Electron System: Theory and Experiment. *J. Am. Chem. Soc.* **1995**, *117*, 5387–5388. [CrossRef]
13. Feixas, F.; Vandenbussche, J.; Bultinck, P.; Matito, E.; Solà, M. Electron Delocalization and Aromaticity in Low-Lying Excited States of Archetypal Organic Compounds. *Phys. Chem. Chem. Phys.* **2011**, *13*, 20690–20703. [CrossRef] [PubMed]
14. Papadakis, R.; Ottosson, H. The Excited State Antiaromatic Benzene Ring: A Molecular Mr Hyde? *Chem. Soc Rev.* **2015**, *44*, 6472–6493. [CrossRef] [PubMed]
15. Stevenson, R.L. *Strange Case of Dr. Jekyll and Mr. Hyde*; Longmans, Green and Co.: London, UK, 1886; ISBN 978-0-553-21277-8.
16. Aihara, J.-I. Aromaticity-Based Theory of Pericyclic Reactions. *Bull. Chem. Soc. Jpn.* **1978**, *51*, 1788–1792. [CrossRef]
17. Fratev, F.; Monev, V.; Janoschek, R. Ab Initio Study of Cyclobutadiene in Excited States: Optimized Geometries, Electronic Tranisitions and Aromaticities. *Tetrahedron* **1982**, *38*, 2929–2932. [CrossRef]
18. Garavelli, M.; Bernardi, F.; Cembran, A.; Castaño, O.; Frutos, L.S.; Merchán, M.; Olivucci, M. Cyclooctatetraene Computational Photo- and Thermal Chemistry: A Reactivity Model for Conjugated Hydrocarbons. *J. Am. Chem. Soc.* **2002**, *124*, 13770–13789. [CrossRef] [PubMed]
19. Villaume, S.; Fogarty, H.A.; Ottosson, H. Triplet-State Aromaticity of $4n\pi$-Electron Monocycles: Analysis of Bifurcation in the π Contribution to the Electron Localization Function. *ChemPhysChem* **2008**, *9*, 257–264. [CrossRef] [PubMed]
20. Sung, Y.M.; Yoon, M.-C.; Lim, J.M.; Rath, H.; Naoda, K.; Osuka, A.; Kim, D. Reversal of Hückel (anti)aromaticity in the Lowest Triplet States of Hexaphyrins and Spectroscopic Evidence for Baird's Rule. *Nat. Chem.* **2015**, *7*, 418–422. [CrossRef] [PubMed]

21. Sung, Y.M.; Oh, J.; Kim, W.; Mori, H.; Osuka, A.; Kim, D. Switching between Aromatic and Antiaromatic 1,3-Phenylene-Strapped[26]- and [28]Hexaphyrins upon Passage to the Singlet Excited State. *J. Am. Chem. Soc.* **2015**, *137*, 11856–11859. [CrossRef] [PubMed]
22. Sung, Y.M.; Oh, J.; Cha, W.-Y.; Kim, W.; Lim, J.M.; Yoon, M.-C.; Kim, D. Control and Switching of Aromaticity in Various All-Aza-Expanded Porphyrins: Spectroscopic and Theoretical Analyses. *Chem. Rev.* **2017**, *117*, 2257–2312. [CrossRef] [PubMed]
23. Wan, P.; Krogh, E. Evidence for the Generationo of Aromatic Cationic Systems in the Excited State. Photochemical Solvolysis of Fluoren-9-ol. *J. Chem. Soc. Chem. Commun.* **1985**, *17*, 1207–1208. [CrossRef]
24. Wan, P.; Krogh, E.; Chak, B. Enhanced Formation of 8π(4*n*) Conjugated Carbanions in the Excited State: First example of Photochemical C–H Bond Heterolysis in Photoexcited State. *J. Am. Chem. Soc.* **1988**, *110*, 4073–4074. [CrossRef]
25. Wan, P.; Budac, D.; Krogh, E. Excited State Carbon Acids: Base Catalysed Photoketonization of Dibenzosuberenol to Dibenzosuberone via Initial C–H Bond Heterolysis from S1. *J. Chem. Soc. Chem. Commun.* **1990**, *3*, 255–257. [CrossRef]
26. Wan, P.; Budac, D.; Earle, M.; Shukla, D. Excited-State Carbon Acid: Photochemical Carbon–Hydrogen Bond Heterolysis vs. Formal di-π-Methane Rearrangement of 5H-Dibenzo[a,c]cycloheptene and Related Compounds. *J. Am. Chem. Soc.* **1990**, *112*, 8048–8054. [CrossRef]
27. Budac, D.; Wan, P. Excited-State Carbon Acid. Facile Benzylic Carbon–Hydrogen Bond Heterolysis of Subrene on Photolysis in Aqueous Solution: A Photogenerated Cyclically Conjugated 8π-electron Carbanion. *J. Org. Chem.* **1992**, *57*, 887–894. [CrossRef]
28. Wan, P.; Shukla, D. Utility of Acid-Base Behavior of Excited States of Organic Molecules. *Chem. Rev.* **1993**, *93*, 571–584. [CrossRef]
29. Mohamed, R.K.; Mondal, S.; Jorner, K.; Delgado, T.F.; Lobodin, V.V.; Ottosson, H.; Alabugin, I.V. The Missing C1–C5 Cycloaromatization Reaction: Triplet State Antiaromaticity Relief and Self-Terminating Photorelease of Formaldehyde for Synthesis of Fulvenes from Enynes. *J. Am. Chem. Soc.* **2015**, *137*, 15441–15450. [CrossRef] [PubMed]
30. Papadakis, R.; Li, H.; Bergman, J.; Lundstedt, A.; Jorner, K.; Ayub, R.; Haldar, S.; Jahn, B.O.; Denisova, A.; Zietz, B.; et al. Metal-free Photochemical Silylations and Transfer Hydrogenations of Benzenoid Hydrocarbons and Graphene. *Nat. Commun.* **2016**, *7*, 12962. [CrossRef] [PubMed]
31. Ueda, M.; Jorner, K.; Sung, Y.M.; Mori, T.; Xiao, Q.; Kim, D.; Ottosson, H.; Aida, T.; Itoh, Y. Energetics of Baird Aromaticity Supported by Inversio of Photoexcited Chiral [4*n*]Annulene Derivatives. *Nat. Commun.* **2017**, *8*, 346. [CrossRef] [PubMed]
32. Zhu, J.; Schleyer, P.R. Evaluation of Triplet Aromaticity by the Isomerization Stabilization Energy. *Org. Lett.* **2013**, *15*, 2442–2445. [CrossRef] [PubMed]
33. An, K.; Zhu, J. Evaluation of Triplet Aromaticity by the Indene-Isoindene Isomerization Stabilization Energy Method. *Eur. J. Org. Chem.* **2014**, *13*, 2764–2769. [CrossRef]
34. Ayub, R.; Papadakis, R.; Jorner, K.; Zietz, B.; Ottosson, H. The Cyclopropyl Group: An Excited State Aromaticity Indicator? *Chem. Eur. J.* **2017**, *23*, 13684–13695. [CrossRef] [PubMed]
35. Ishikawa, M.; Naka, A.; Kobayashi, H. The Chemistry of Silacyclobutene: Synthesis, Reactions, and Theoretical Study. *Coord. Chem. Rev.* **2017**, *335*, 58–75. [CrossRef]
36. Tzeng, D.; Fong, R.H.; Dilanjan, H.S.; Weber, W.P. Evidence for the Intermediacy of 1,1-dimethyl-2-phyenyl-1-sila-1,3-butadiene in the Photochemistry and Pyrolysis of 1,1-dimethyl-2-phenyl-1-sila-2-cyclobutene. *J. Organomet. Chem.* **1981**, *219*, 153–161. [CrossRef]
37. Carey, F.A.; Sundberg, R.J. *Advanced Organic Chemistry. Part A: Structure and Mechanisms*, 5th ed.; Springer: New York, NY, USA, 2007.
38. Mauksch, M.; Tsogoeva, S.B. A Preferred Disrotatory 4*n* Electron Möbius Aromatic Transition State for a Thermal Electrocyclic Reaction. *Angew. Chem. Int. Ed.* **2009**, *48*, 2959–2963. [CrossRef] [PubMed]
39. Brink, M.; Möllerstedt, H.; Ottosson, C.-H. Characteristics of the Electronic Structure of Diabatically and Adiabatically *Z*/*E*-Isomerizing Olefins in the T_1 state. *J. Phys. Chem. A* **2001**, *105*, 4071–4083. [CrossRef]
40. Villaume, S.; Ottosson, H. Aromaticity Changes along the Lowest-Triplet State Path for C=C Bond Rotation of Annulenyl-Substituted Olefins Probed by Electron Localization Function. *J. Phys. Chem. A.* **2009**, *113*, 12304–12310. [CrossRef] [PubMed]

41. Zhu, J.; Fogarty, H.A.; Möllerstedt, H.; Brink, M.; Ottosson, H. Aromaticity Effects on the Profiles of the Lowest Triplet-State Potential-Energy Surfaces for Rotation about the C=C Bonds of Olefins with Five-Membered Ring Substituents: An Example of the Impact of Baird's Rule. *Chem. Eur. J.* **2013**, *19*, 10698–10707. [CrossRef] [PubMed]
42. Kato, H.; Brink, M.; Möllerstedt, H.; Piqueras, M.C.; Crespo, R.; Ottosson, H. *Z*/*E*-Photoisomerizations of Olefins with $4n\pi$-or $(4n + 2)\pi$-Electron Substituents: Zigzag Variations in Olefin Properties along the T1 state Potential Energy Surfaces. *J. Org. Chem.* **2005**, *70*, 9495–9504. [CrossRef] [PubMed]
43. Ottosson, H.; Eklöf, A.M. Silenes: Connectors between Classical Alkenes and Nonclassical Heavy Alkenes. *Coord. Chem. Rev.* **2008**, *252*, 1287–1314. [CrossRef]
44. Kang, K.T.; Yoon, U.C.; Seo, H.C.; Kim, K.N.; Song, H.Y.; Lee, J.C. Thermal and Photochemical Reactions of Benzosilacyclobutenes with Alcohols. Intermediaxy of *o*-Silaquinone Methide in the Photochemical Reactions. *Bull. Korean Chem. Soc.* **1991**, *12*, 57–60.
45. Bendikov, M.; Quadt, S.R.; Rabin, O.; Apeloig, Y. Addition of Nucleophiles to Silenes. A Theoretical Study of the Effect of Substituents on Their Kinetic Stability. *Organometalllics* **2002**, *21*, 3930–3939. [CrossRef]
46. Kang, K.T.; Seo, H.C.; Kim, K.N. Thermal Reactions of Benzosilacyclobutenes with Alcohols. *Tetrahedron Lett.* **1985**, *26*, 4761–4762. [CrossRef]
47. Walsh, R. Bond Dissociation Energy Values in Silicon-Containing Compounds and Some of their Implications. *Acc. Chem. Res.* **1981**, *14*, 246–252. [CrossRef]
48. McMillen, D.F.; Golden, D.M. Hydrocarbons Bond Dissociation Energies. *Ann. Rev. Phys. Chem.* **1982**, *33*, 493–532. [CrossRef]
49. Segura, J.L.; Martín, N. *o*-Quinodimethanes: Efficient Intermediates in Organic Synthesis. *Chem. Rev.* **1999**, *99*, 3199–3246. [CrossRef] [PubMed]
50. Ishikawa, M.; Naka, A.; Yoshizawa, K. The Chemistry of Benzodisilacyclobutenes and Benzobis(disilacyclobutene)s: New Development of Transition-Metal-Catalyzed Reactions, Stereochemistry and Theoretical Studies. *Dalton Trans.* **2016**, *45*, 3210–3225. [CrossRef] [PubMed]
51. Taubert, S.; Sundholm, D.; Jusélius, J. Calculations of Spin-Current Densities Using Gauge-Including Atomic Orbitals. *J. Chem. Phys.* **2011**, *134*, 54123–54135. [CrossRef] [PubMed]
52. Soncini, A.; Fowler, P.W. Ring-Current Aromaticity in Open-Shell Systems. *Chem. Phys. Lett.* **2008**, *450*, 431–436. [CrossRef]
53. Jursic, B.S. Exploring the lowest energy triplet potential energy surface for cyclic c_4h_4 isomers with the complete basis set ab initio method. Is the transformation of triafulvene into cyclobutadiene possible in their excited states? *J. Mol. Struct. (THEOCHEM)* **1999**, *490*, 133–144. [CrossRef]
54. Brook, M.A. *Silicon in Organic, Organometallic, and Polymer Chemistry*; John Wiley and Sons: Hoboken, NJ, USA, 2000; ISBN 0-471-19658-4.
55. Zamstein, N.; Kallush, S.; Segev, B. A phase-space approach to the $T_1 \rightsquigarrow S_0$ radiationless decay in benzene: The effect of deuteration. *J. Chem. Phys.* **2005**, *123*, 074304. [CrossRef] [PubMed]
56. Schaffroth, M.; Gershoni-Poranne, R.; Stanger, A.; Bunz, U.H.F. Tetraazaacenes Containing Four-Membered Rings in Different Oxidation States. Are They Aromatic? A Computational Study. *J. Org. Chem.* **2014**, *79*, 11644–11650. [CrossRef] [PubMed]
57. Schleyer, P.R.; Pühlhofer, F. Recommendations for the Evaluation of Aromatic Stabilization Energies. *Org. Lett.* **2002**, *4*, 2873–2876. [CrossRef] [PubMed]
58. Breslow, R.; Chang, H.W.; Hill, R.; Wasserman, E. Stable Triplet States of Some Cyclopentadienyl Cations. *J. Am. Chem. Soc.* **1967**, *89*, 1112–1119. [CrossRef]
59. Saunders, M.; Berger, R.; Jaffe, A.; McBride, J.M.; O'Neill, J.; Breslow, R.; Hoffman, J.M., Jr.; Perchonock, C.; Wasserman, E.; Hutton, R.S.; et al. Unsubstituted Cyclopentadienyl Cation, a Ground-State Triplet. *J. Am. Chem. Soc.* **1973**, *95*, 3017–3018. [CrossRef]
60. Wörner, H.J.; Merkt, F. Photoelectron Spectroscopic Study of the First Singlet and Triplet States of the Cyclopentadienyl Cation. *Angew. Chem. Int. Ed.* **2006**, *45*, 293–296. [CrossRef] [PubMed]
61. Wörner, H.J.; Merkt, F. Diradicals, Antiaromaticity, and the Pseudo-Jahn–Teller Effect: Electronic and Rovibronic Structures of the Cyclopentadienyl Cation. *J. Chem. Phys.* **2007**, *127*, 34303. [CrossRef] [PubMed]
62. Frisch, M.J.; Trucks, G.W.; Schlegel, H.B.; Scuseria, G.E.; Robb, M.A.; Cheeseman, J.R.; Scalmani, G.; Barone, V.; Mennucci, B.; Petersson, G.A.; et al. *Gaussian 09, Revision D.01*; Gaussian, Inc.: Wallingford, CT, USA, 2009.

63. Stephens, P.J.; Devlin, F.J.; Chabalowski, C.F.; Frisch, M.J. Ab Initio Calculations of Vibrational Absorption and Circular Dichorism Spectra Using Density Functional Force Fields. *J. Phys. Chem.* **1994**, *98*, 11623–11627. [CrossRef]
64. Becke, A.D. A New Mixing of Hartree–Fock and Local-Density-Functional Theories. *J. Chem. Phys.* **1993**, *98*, 1372–1377. [CrossRef]
65. Handy, N.C.; Cohen, A.J. Left-Right Correlation Energy. *Mol. Phys.* **2001**, *99*, 403–412. [CrossRef]
66. Parr, R.G.; Yang, W. *Density-Functional Theory of Atoms and Molecules*; Oxford University Press: Oxford, UK, 1989.
67. Rrishnan, R.; Binkley, J.S.; Seeger, R.; Pople, J.A. Self-Consistent Molecular Orbital Methods. XX. A Basis Set for Correlated Wave Functions. *J. Chem. Phys.* **1980**, *72*, 650–654. [CrossRef]
68. McLean, A.D.; Chandler, G.S. Contracted Gaussian Basis Sets for Molecular Calculations. I. Second Row Atoms, Z = 11–18. *J. Chem. Phys.* **1980**, *72*, 5639–5648. [CrossRef]
69. Schleyer, P.R. Introduction: Aromatcitiy. *Chem. Rev.* **2001**, *101*, 1115–1118. [CrossRef] [PubMed]
70. Krygowski, T.M. Crystallographic Studies of Inter- and Intramolecular Interactions Reflected in Aromatic Character of π-Electron Systems. *J. Chem. Inf. Comput. Sci.* **1993**, *33*, 70–78. [CrossRef]
71. Stanger, A. Nucleus-Independent Chemical Shifts (NICS): Distance Dependence and Revised Criteria for Aromaticity and Antiaromaticity. *J. Org. Chem.* **2006**, *71*, 883–893. [CrossRef] [PubMed]
72. Stanger, A. Obtaining Relative Induced Ring Currents Quantitatively from NICS. *J. Org. Chem.* **2010**, *75*, 2281–2288. [CrossRef] [PubMed]
73. Rahalkar, A.; Stanger, A. Aroma. Available online: http://schulich.technion.ac.il/Amnon_Stanger.htm (accessed on 22 November 2015).
74. Cheeseman, J.R.; Trucks, G.W.; Keith, T.A.; Frisch, M.J. A Comparison of Models for Calculating Nuclear Magnetic Resonance Shielding Tensors. *J. Chem. Phys.* **1996**, *104*, 5497–5509. [CrossRef]
75. Herges, R.; Geuenich, D. Delocalization of Electrons in Molecules. *J. Phys. Chem. A* **2001**, *105*, 3214–3220. [CrossRef]
76. Geuenich, D.; Hess, K.; Kohler, F.; Herges, R. Anisotropy of the Induced Current Density (ACID), a General Method to Quantify and Visualize Electronic Delocalization. *Chem. Rev.* **2005**, *105*, 3758–3772. [CrossRef] [PubMed]
77. Keith, T.A.; Bader, R.F.W. Calculations of Magnetic Response Properties Using a Continuous Set of Gauge Transformations. *Chem. Phys. Lett.* **1993**, *210*, 223–231. [CrossRef]
78. Yan, D.; Mohsseni-Ala, J.; Auner, N.; Bolte, M.; Bats, J.W. Molecular Optical Switches: Synthesis, Structure, and Photoluminescence of Spirosila Compounds. *Chem. Eur. J.* **2007**, *13*, 7204–7214. [CrossRef] [PubMed]